Fast, accurate, robust and Open Source Brain Extraction Tool (OSBET)

R. Namias[a], P. Donnelly Kehoe[b], J.P. D'Amato[c] and J. Nagel[d]
[a]Machine Learning and Applications Group, CIFASIS-CONICET, Rosario, Argentina.
[b]Laboratory for System Dynamics and Signal Processing, Universidad Nacional de Rosario, CIFASIS-CONICET, Rosario, Argentina.
[c]PLADEMA Institute, Universidad Nacional del Centro, Tandil, Argentina.
[d]Neurorradiology Service, Instituto Gamma, Rosario, Argentina.

ABSTRACT

The removal of non-brain regions in neuroimaging is a critical task to perform a favorable preprocessing. The skull-stripping depends on different factors including the noise level in the image, the anatomy of the subject being scanned and the acquisition sequence. For these and other reasons, an ideal brain extraction method should be fast, accurate, user friendly, open-source and knowledge based (to allow for the interaction with the algorithm in case the expected outcome is not being obtained), producing stable results and making it possible to automate the process for large datasets. There are already a large number of validated tools to perform this task but none of them meets the desired characteristics. In this paper we introduced an open source brain extraction tool (OSBET), composed of four steps using simple well-known operations such as: optimal thresholding, binary morphology, labeling and geometrical analysis, that aims to assemble all the desired features. We present an experiment comparing OSBET with other six state-of-the-art techniques against a publicly available dataset consisting of 40 T_1-weighted 3D scans and their corresponding manually segmented images. OSBET gave both: a short duration with an excellent accuracy, getting the best Dice Coefficient metric. Further validation should be performed, for instance, in unhealthy population, to generalize its usage for clinical purposes.

Keywords: Skull-stripping, Magnetic Resonance Imaging, Neuroscience

1. INTRODUCTION

The removal of non-brain regions from neuroimages is a very important task required for many complex algorithms used in medical practices such as automatic segmentation, volume analysis, registration and even in visualization. This stage, generally called brain extraction or skull-stripping, is frequently performed in T1-weighted magnetic resonance images (MRIs).

An important number of different techniques have been developed to accomplish this task in the most effective and accurate way.[1,2] Previous studies have compared the performance of the most commonly used brain extraction methods (generally called BEMs) and concluded that existing algorithms had both strengths and weaknesses.[3–7] The most widely used **BEMs** are FSL's Brain Extraction Tool (BET),[8] Statistical Parameter Mapping (SPM) in its multiples versions,[9] Model-based Level Sets (MLS)[10] and FreeSurfer's Hybrid Watershed Algorithm (HWA).[11] These well-known tools still have some issues to overcome in order to get an ideal **BEM**.

An ideal open-source Brain Extraction Method should be fast, accurate and user friendly, and it also must require minimal user configuration to produce automatic and stable results, even when large datasets are processed. Therefore, in this paper we introduce a novel method that overfills these requirements. We summarized the experimental results, evaluation, and comparison of our method to six of the most used BEMs including BET, SPM and MLS; finally, we discuss the advantages and disadvantages of our method for brain MRI extraction.

1.1 State-of-the-art methods

We review six of the most used open-source BEMs. All of them are publicly available and include the cerebellum and brainstem in the segmentation:

- *FSL's Brain Extraction Tool (BET):*[8] this part of FSL package uses a deformable model initialized as a spherical mesh around the center of gravity of the head image and gradually grows using triangular tessellation of the mesh surface. BET is very fast and relatively insensitive to parameter settings, providing good results considering its simplicity. The standard usage usually produces false positive errors around the brainstem that can be solve by using a processing pipeline that consists of, 1) Running BET, then 2) registering the resulting image to an atlas and finally 3) running BET again. Although this method corrects this high false positive rate, it prolongs significantly the processing time as we will observe in the results section. A weakness of FSL's BET is needing a prior removal of the neck in order to gather accurate results.[12]

- *Model-based Level Sets (MLS):*[10] as its name indicates this is an application that implements a mathematical algorithm using a model-based level set where the evolution of the curve is controlled by two terms in the level set equation. The values of these terms represent forces that determine the speed of the evolving curve. The first force is derived from the mean curvature of the curve, and the second is designed to model the intensity characteristics of the cortex in MR images. The combination of these forces push or pull the curve toward the brain surface.

- *Statistical Parameter Mapping (SPM):*[9] this is a MATLAB software that allows processing neuroimages in a broad spectrum, including segmentation, registration and functional MRI(fMRI). In this work we have used SPM v12 to perform skull-stripping and as we expected, by the fact that it was developed in MATLAB, the main disadvantage is that it consumes a significant amount of time. Also skull-stripping using SPM is not a trivial process because is should be performed in 2 steps. First, the user has to generate, from the original image (O_i), the probability maps of white matter (P_w) and gray matter (P_g), by using the segmentation tool spm_imcalc. Then, the second step consists on making a thresholded arithmetical operation, denoted by ($\bullet$) in Eq. 1, among these three entities as it is described in Eq. 1, where B_i is the brain image and T_h the threshold value which should be manually defined. This final step is performed using the spm_imcalc's module which allows to perform arithmetical operations between images. In summary, the procedure not only has a free parameter but also two steps that are not trivial for someone who is not familiar with the application. In addition, the processing time, as we will describe later, is also another downside of SPM's skull stripping.

$$B_i = O_i \bullet ((P_w + P_g) > T_h) \tag{1}$$

- *AFNI:*[13] this software contains the package 3dSkullStrip, that combined with another AFNI's package(3dcalc) can provide a skull stripping that is based in the same concepts that BET uses, but with some modifications. According to the authors,[14] these differences include avoiding eyes and ventricles, reducing leakage into the skull and using also data outside the surface (and not only inside) to guide the evolution of the surface, among others.

- *Skull-stripping filter for ITK:*[15] this is an open-source BEM that was developed using the library ITK and it is based on a two step procedure. It starts by registering the image to an atlas, using an affine transformation model and then the brain mask of the atlas is propagated to the patient's image with the calculated transformation matrix. The second step is to erode the brain mask and then enhance it using a refined brain extraction based on level-sets.

- *ROBEX:*[12] this system uses a hybrid solution that combines a discriminative model and a generative model in order to perform the brain extraction. The discriminative model is a Random Forest classifier trained to detect the brain boundary and the generative model is a point distribution model that ensures that the result is plausible. When a new image is presented to the system, the generative model is used to search for the contour with highest likelihood according to the discriminative model. Because the target shape is in general not perfectly represented by the generative model, the contour is refined using graph cuts to obtain the final segmentation. The main disadvantage of this BEM is that it uses an atlas-based segmentation, that depends on the result of a registration.

We summarize the main characteristics of the above described methods, along with data from an exploratory analysis collected by the authors as end-users, in Table 1. It can be seen that each of these methods fails, at least, in one of the ideal features. For this reason we aimed to develop an open-source *high performance* parameter-free BEM, that could be used in a simple way, producing robust results. In order to keep the design as simple as possible, we made OSBET atlas independent (avoiding registration), using simple and fast image processing techniques while keeping a low computational cost.

Table 1. Comparative of different open source BEMs obtained by exploratory analysis.

Method	Requirements/Limitations	Speed	User friendly	Parameters needed
BET	Neck removal is needed Atlas alignment is advised	Fast	Good	Optional
MLS		Average	Average	Yes
SPM	Atlas based (orientation dependent)	Slow	Not trivial	Yes
AFNI	Neck removal is advised	Average	Average	Yes
ITK-Filter	Atlas based (orientation dependent)	Slow	Not trivial	No
ROBEX	Atlas based (orientation dependent)	Average	Average	No

2. METHOD

The OSBET method is a full 3D enhanced version of the one proposed by Somansundaram and Kalaiselvi.[7] It is compound of four steps, in contrast to the two stage original procedure. In first place, a rough brain mask extraction using a tissues labeling procedure based on their signal intensity level is performed. Secondly, a histogram-based filter removes most of the optical nerves in order to avoid false positives in the subsequent morphological segmentation. In third place, a complete 3D morphological segmentation is ran including a connected component filtering. Finally, we have used a 2D hole-filling step that recovers voxels that could have been left out in the segmentation step. The OSBET method was implemented in C++, as a set of new ITK filters. A distribution code can be downloaded from `http://www.cifasis-conicet.gov.ar/namias/Files/Filters/OSBET.tar.gz`.

2.1 Labeling and rough brain detection

The first step process stages, which are summarized in Fig. 1, consists in three-sub-steps. Each one, deals with the labeling of different tissues and organs.

Head contour mask The first step starts by applying an optimal iterative thresholding technique proposed by Ridler[16] to the input image (O_i). The optimal threshold value T_{op} is iteratively computed as follows:

$$T^{t+1} = \frac{\mu_{bg}^t + \mu_{fg}^t}{2} \tag{2}$$

where μ_{bg}^t and μ_{fg}^t are the mean background (bg) and foreground (fg) signal intensity at iteration t, respectively. Afterwards, we binarize the image O_i by applying a thresholding operation keeping the voxels $I(x, y, z) \geq T_{op}$. The resulting volumetric mask (M_t) is then labeled using a ray-cast technique in the x and y axes. In each slice corresponding to a z plane, one x-ray and one y-ray iterates over each row and column respectively searching for the first $[0, 1]$ voxel values sequence (outside-inside) and the last $[1, 0]$ voxel value sequence (inside-outside). Therefore, each ray will mark the beginning and the ending of the skull in the x and y directions. All the voxels inside the resulting skull limit will be set to 1 defining the head mask M_h.

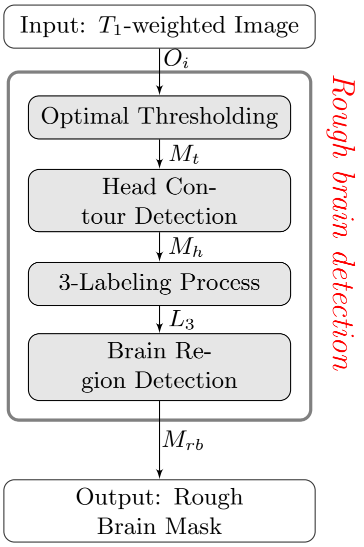

Figure 1. Flowchart of 1^{st}step: rough brain detection.

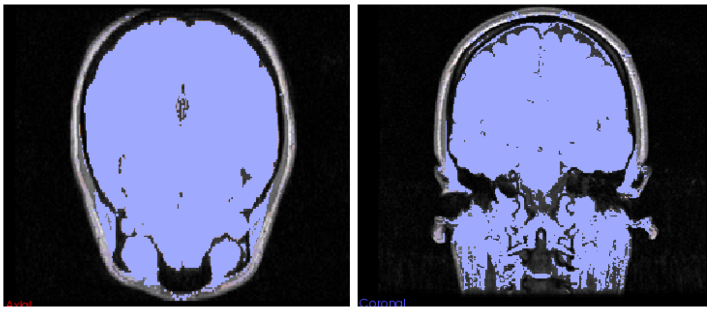

Figure 2. 1^{st}step example: Rough brain mask (M_{rb}). Axial and coronal views.

3-Labeling process Combining M_t and M_h, we proceed to identify the inner dark region representing the skull and the cerebrum-spinal fluid (CSF) with the label 2. The output is a 3-labeled volumetric mask (L_3):

$$L_3(x,y,z) = \begin{cases} 0 & \text{if } M_t(x,y,z) = 0 \text{ and } M_h(x,y,z) = 0 \\ 1 & \text{if } M_t(x,y,z) = 1 \\ 2 & \text{if } M_t(x,y,z) = 0 \text{ and } M_h(x,y,z) = 1 \end{cases} \tag{3}$$

Now, we have L_3 with the voxels in the background labeled as 0. The voxels in the the scalp and brain tissues labeled as 1, and the remaining voxels representing the skull, the CSF, and others., labeled as 2.

Brain region detection To obtain a rough brain portion, a run-length identification scheme for labeling is employed[17] over the 3-labeled volumetric mask L_3. We look for runs of 1's beginning and ending with 2's (R_{bt}) which represent brain tissues. Hence, we make the identification over the three axes of the image, gathering the rough brain mask:

$$M_{rb} = \begin{cases} M_h(x,y,z) & \text{if } (x,y,z) \in R^d_{bt} \\ 0 & \text{otherwise} \end{cases} \tag{4}$$

where $R^d_{bt} = R^x_{bt} \cup R^y_{bt} \cup R^z_{bt}$ represents one a voxel belonging to a R_{bt} run in any of the three directions $d = \{x, y, z\}$.

The resulting M_{rb} has leftover regions which will be afterwards removed in the morphological segmentation step (Fig. 2). Nevertheless, there is an specific region which is hard to isolate using morphological operations,

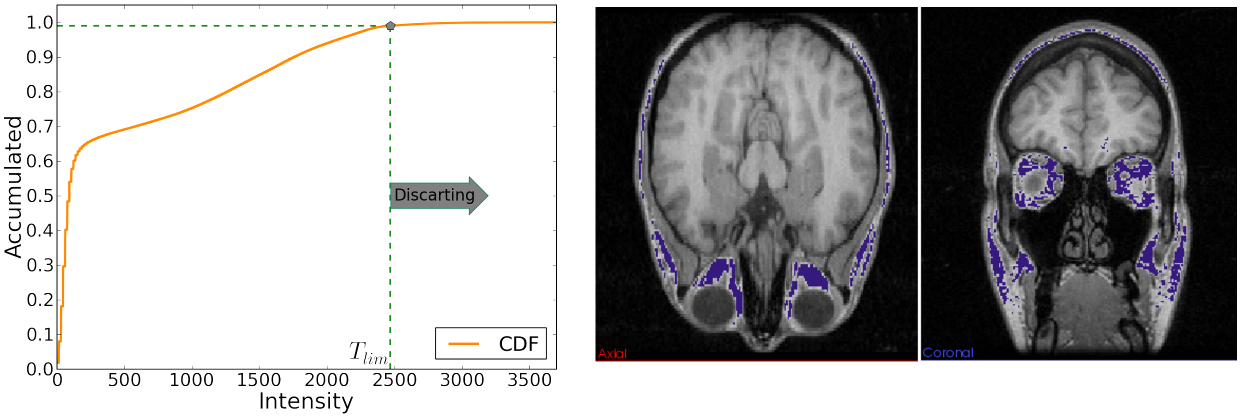

(a)

(b)

Figure 3. 2^{nd}step example: Optical nerve extraction. (a) Automatic T_{lim} value from the CDF. (b) Resulting mask (M_{op})(dark-violet): axial and coronal views.

the optical nerves. These nerves have a characteristic hyper intensity in T1-weighted images, very similar to the brain tissue. For this reason, they are unlikely to be detached from the brain portion in the M_{rb} (bottom left, Fig. 2).

2.2 Eyes and optic nerve extraction

The second step deals with the optical nerve removal from the rough brain mask in order to avoid false positives in the final result. This filtering step takes advantage of the fact that optical nerves have a hyper-intense signal in T_1-weighted images. We compute the cumulative distribution function (CDF) from the image histogram and choose the $T_{lim} = \text{CDF}(x \geq 0.99)$ (Fig. 2.2). Then, we extract the optical nerve volumetric mask (M_{op}) using a binary thresholding with $T = T_{lim}$ (Fig 2.2). Finally, we obtain the enhanced rough brain mask (M'_{rb}) by extracting M_{op} from the rough brain mask: $M'_{rb} = M_{rb} - M_{op}$.

2.3 Morphological segmentation

The goal of the morphological segmentation step is to obtain a brain mask (M_{br}) from the enhanced rough brain mask M'_{rb} acquired from the previous step. An asynchronous asymmetric morphological 3D opening (erosion and dilation) is performed, with a connected component filtering operation in-between (Fig. 4).

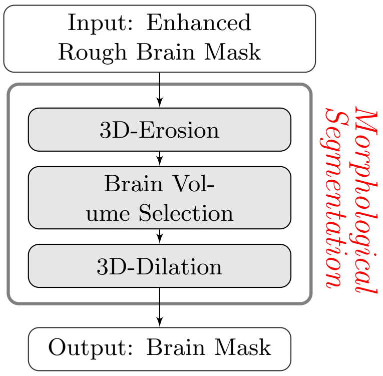

Figure 4. Flowchart of 3^{rd}step: morphological segmentation.

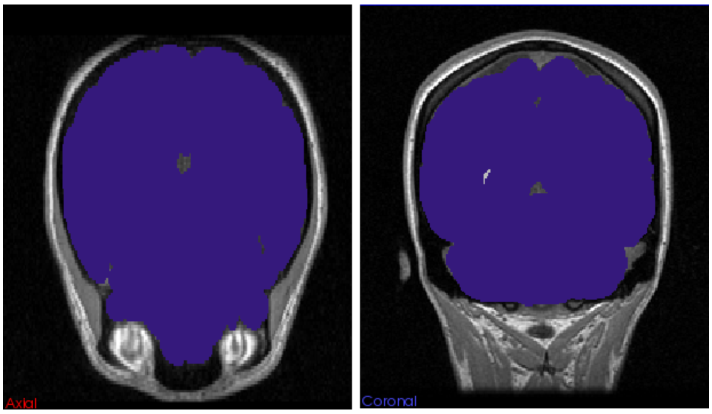

Figure 5. 3^{rd}step example: Morphological segmentation mask (M_{br}). Axial and coronal views.

3D-Erosion The enhanced mask M'_{rb} is eroded by a ball-shaped structuring element with radius: 4 ($9 \times 9 \times 9$ voxels). After the erosion, the resulting volumetric mask should have a set of disconnected regions ($R_i, i = 1 \ldots n$). These disconnected regions are labeled using a classical connected component labeling technique.

Brain volume selection The next step is to select the brain region from all the disconnected R_i. Therefore, we compute the regions volumes $V(R_i), i = 1 \ldots n$ and then select the largest region (R_l):

$$R_l = \max_{i=1..n} V(R_i) \tag{5}$$

where R_l represents the eroded brain mask M_{er}.

3D-Dilation The complete segmentation step is an asynchronous asymmetric morphological 3D opening operation. To obtain better quality results, we used a larger ball-shaped structuring element in the dilation operation with radius: 5 ($11 \times 11 \times 11$ voxels). After the dilation operation we have the brain mask (M_{br}). Although the brain mask has a smooth border, sometimes it presents inner holes which are filled in the final step (Fig. 5) .

2.4 Hole-filling

The final hole-filling step uses a slice-by-slice binary hole filling ITK filter.[18] Although this filter works on 3D images, it is not convenient to use it in the volumetric configuration since it does not fill the inner regions which are connected to the outside. For this reason, we use an axial slice-by-slice 2D hole-filling filtering (Fig. 6). Summarizing, in this final step, the final mask M_f is obtained by applying the slice-by-slice hole-filling filter to the M_{br}. Figure 7 shows, in pink, the completed regions.

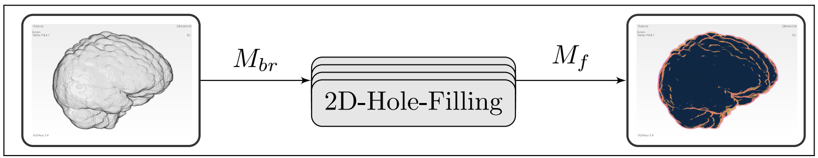

Figure 6. Flowchart of 4^{th}step: Hole-filling.

3. VALIDATION

3.1 Dataset

The used dataset is the LONI Probabilistic Brain Atlas (LPBA40),[19] which is publicly available in `http://sve.loni.ucla.edu/`. It consists in 40 T_1-weighted scans (20 males, 20 females, age 29.24±6.30 years) and

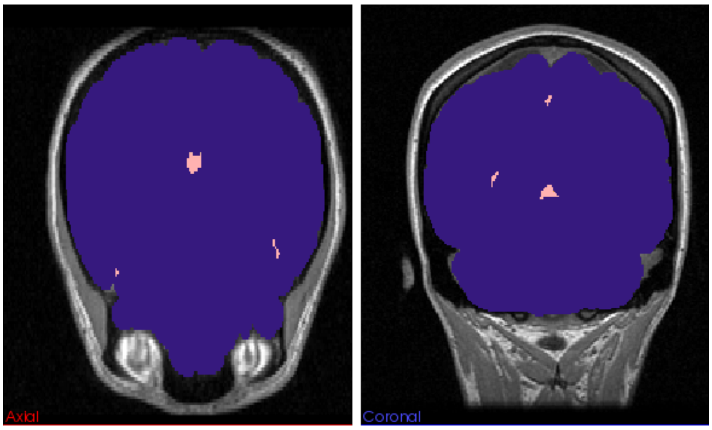

Figure 7. 4^{th}step example: Hole-filling mask (M_f). Filled holes (pink) over M_{br} (dark-violet). Axial and coronal views.

their corresponding annotations. The scans were acquired with a High-resolution 3D Spoiled Gradient Echo (SPGR) on a General Electrics (GE) 1.5T system. The acquisition parameters were: TR: 10.0-12.5 ms; TE range 4.22-4.5 ms; flip angle 20°. Coronal slices were acquired 1.5 mm apart with in-plane resolution of 0.86 mm (38 subjects) or 0.78 mm (2 subjects). Each MRI was manually skull-stripped and segmented by experts to identify a set of 56 structures in the brain.

3.2 Comparison Process

The proposed method was compared with BEMs described in 1.1, with no preprocessing taking place before feeding the images to the BEMs. For the methods requiring parameter tuning, the best available configuration (according to the bibliography) was used.
In the case of BET, two different configurations were tested:

- *Fast BET:* This configuration performed a standard BET's brain extraction, using the fractional intensity threshold equal to 0.5.
- *BET's authors suggestion (BET-AS):* This was the suggested configuration of BET's authors based on,[14] and consisted in one iterative brain extraction, followed by an alignment to an atlas, with a final iterative brain extraction. This method increased the computational cost, and consequently the processing time.

According to BET's authors,[14] they also requested a previous removal of the neck. This requirement was not accepted by the present authors, given that, in order to call a BEM as robust, its performance does not have to be affected by the presence of the neck in the MR image.
For AFNI's 3dSkullStrip, two configurations were tested also:

- *Default:* A standard skull-stripping was performed using the default parameters.
- *AFNI's authors suggestion (AFNI-AS):* consisting in setting two parameters in a non standard value, particularly *shink_fac_bot_lim=0.65* and *shink_fac=0.72*.[14]

Automatically segmented brains were compared with the manually-segmented ones to quantify the effectiveness of each BEM. Selected metrics aimed to give an objective score of precision, robustness and velocity, consisted of:

- *Sorensen-Dice coefficient (DC):* This coefficient's value ranges between 0 and 1 and represents in which sets A and B are similar:
$$D(A,B) = \frac{2|A \cap B|}{|A| + |B|} \tag{6}$$
One weakness of this coefficient is that small meaningful volumes can be underestimated, because this score assumes that all voxels have the same weight.

- *False positives (FP):* indicates which proportion of all the voxels classified as brain-voxels were mistaken.
- *False negatives (FN):* shows which proportion of all the voxels classified as non brain-voxels were mistaken.
- *Hausdorff distance (HD):* is the maximum deviation in mm from the reference mask.[20]
- *Specificity (S_p):* measures the proportion of negatives (not-brain voxels) which are correctly identified.
- *Sensitivity (S):* measures the proportion of actual positives (brain voxels) which are correctly identified.
- *Average duration (AD):* measures how much time per volume each algorithm takes.

The ideal BEM must have DC, S and Sp equal to 1,and consequently FP and FN should be 0. The AD should be as short as possible.

4. RESULTS

We performed an experiment by applying our OSBET and the other BEMs shown in Section 1.1 to 40 head scans from the LPBA dataset and performed a quantitative analysis. BET and AFNI's BEM were tested in two different configurations, as explained in Section 3, the sufix AS means author's suggestion henceforth. In first place, we selected DC, HD and AD as main indicators to analyze the performance of the BEMs. Table 2 shows the comparative analysis of the 7 tested BEMs, with two different configurations for BET and AFNI. There we can observe that OSBET got the best DC, meaning that, up to some extent under these experiment condition, it is the most accurate skull-stripping method. Also this is reinforced by a good HD. When analyzing the computational cost and therefore the AD of the skull-stripping, OSBET was the 2^{nd} fastest BEM, and should be noted that no optimization nor parallelization was performed in the code. The mean time of BET was 2.72 ± 0.850 while for OSBET was 4.28 ± 0.146, meaning that although in average BET was faster, OSBET had less dispersion in the AD.

Interestingly the worst performance was presented by the other ITK-based BEM (beside OSBET), this ITK-Filter obtained a DC of 0.910 and a very long AD, showing us that it is not fast nor robust and not even easy to use, given that it uses an atlas that we had to reorient in order to be aligned to our images in the first place so that this BEM could work properly. SPM's brain extraction obtained the smallest HD, but the time used per volume makes it not convenient for large datasets. BET-AS has improved BET performance but at the expense of increasing the processing duration up to a mean of 65.29 seconds per volume. MLS algorithm presented an easy implementation and a good overall result, but sadly it shown some leaks that increment significantly the HD. AFNI-AS has proven to be a very robust BEM with high DC, low HD and a regular AD.

In the case of ROBEX we first tested the version 1.2, available in `http://wwww.nitrc.org/projects/robex`, but we realized that it has a bug in the registration. After checking this with the authors, they told us that the registration has been changed between version 1.0[12] and version 1.2. For this reason, we finally decided to use ROBEX v1.0 and, as can be seen in Table 2, it showed a very good performance. The disadvantages we found are that ROBEX v1.0 does not accept or deliver NIFTI images and that input images have to be oriented in the same way that the used atlas has. As for its usability, it is very simple to use and does not require any parameter tuning.

After this main analysis, we selected two secondary indicators, which are S and S_p, that show us which trend each BEM have, that is to say, if a particular BEM is more accurate in detecting brain voxels (high S), most of the times at the expense of an over-segmentation (low S_p) or if a BEM if more accurate in detecting not-brain voxels (high S_p), frequently performing an under-segmentation (low S). Table 3 shows the results obtained by this secondary analysis, where we can observe which methods have a balanced behavior. In the case of standard BET we see that it has the highest S, but lowest S_p, meaning that is over-segmenting, while for the BET-AS the S is considerable low, while the S_p very high, performing an under-segmentation. In SPM,MLS, ROBEX and OSBET both values are balanced. AFNI's segmentation has low S and S_p, meaning that is a bad BEM, while in the case of AFNI-AS, S_p have an acceptable value but the S is low, meaning that is performing an under-segmentation. The ITK-Filter is performing a gross under-segmentation.

Table 2. Comparative analysis of different available BEMs using DC, HD and AD as main indicators. The proposed method (OSBET) has the highest DC, the smallest 4^{rd} HD and the smallest 2^{nd} AD.

Method	Dice Coefficient	Hausdorff Distance[mm]	Average duration[s]
BET	0.945±0.032	28.54±10.93	**2.72**
BET-AS	0.951±0.022	20.06±9.16	65.29
SPM	0.952±0.020	**11.19**±2.65	210.10
MLS	0.957±0.022	30.02±17.45	51.86
AFNI	0.936±0.026	23.48±13.04	58.59
AFNI-AS	0.954±0.007	13.70±2.96	52.21
ITK-Filter	0.910±0.017	14.92±3.50	311.84
ROBEX	0.966±0.003	12.18±3.94	60.40
OSBET	**0.968±0.012**	13.83±5.19	4.28

Table 3. Comparative analysis of deferents available BEMS using S and S_p as indicators. The proposed method (OSBET) has best overall efficacy, maintaining both coefficients high. Should be noted that others BEMs have high S at the expense of a low S_p and vice versa.

Method	Sensitivity (S)	Specificity (S_p)
BET	$\mathbf{0.985 \pm 0.006}$	0.982 ± 0.014
BET-AS	0.917 ± 0.042	$\mathbf{0.998 \pm 0.001}$
SPM	0.969 ± 0.011	0.988 ± 0.009
MLS	0.957 ± 0.015	0.992 ± 0.008
AFNI	0.959 ± 0.010	0.983 ± 0.011
AFNI-AS	0.958 ± 0.009	0.991 ± 0.004
ITK-Filter	0.860 ± 0.037	0.995 ± 0.006
ROBEX	0.958 ± 0.009	0.995 ± 0.011
OSBET	0.964 ± 0.027	0.995 ± 0.002

We want to highlight OSBET's performance, that we believe is in a perfect balance between under-segmentation and over-segmentation, therefore it can be seen as a good BEM, and considering that is very fast and no configuration parameters are needed, we have to say that (in our opinion and for this dataset) it is the best BEM available.

The experiments were ran in an Intel(R) Core(TM) i5-3570 CPU @ 3.40GHz with 16Gb RAM and Linux kernel version: 3.11.0-26-generic.

5. CONCLUSION

In this paper a new fully automated 3D skull-stripping method has been presented. The objectives of the design were to seek for an ideal BEM, defining it as open source, fast, accurate, robust, with no parameter tuning required, allowing to process a large amount of MRIs. The proposed method is a four step procedure based on a 3D T1-weighted head MRI. In the first step a labeling and rough brain extraction is performed, then an eye and optic nerve extraction is done and finally a morphological segmentation and hole-filling is carried out.

This developed method, called OSBET, was validated with a public database of 40 head MRIs. During the testing, OSBET was compared with a selection of six of the most used BEMs and in two of them (BET and AFNI's brain extractor) two different configurations has been tried. The experimental evaluation in this paper is based only on publicly accessible BEMs and data, so all experiments can be reproduced.

In order to quantify the results three main parameter were selected, DC, HD and AD; and two secondary indicators, S and Sp. OSBET obtained the best DC with a value of 96.8%, followed by ROBEX with 95.9%, also it got one of the smallest HD with 13.83 mm, while the best rated for this indicator was SPM with 11.19 mm. Interestingly OSBET was one of the only two methods getting an AD less that 10 seconds, with a mean of 4.28 seconds. With respect to the secondary indicators, most of the methods obtained either a good S and a bad Sp or vice versa, while OSBET was one of the few, along with MLS, SPM and ROBEX that exhibited a balanced behavior.

Compared with other methods, OSBET is an interesting alternative that combines several desirable features, is very fast, accurate, easy to use and open-source. It does not use any atlas, becoming independent of the orientation in the input images and avoiding problems in the registration.

The next step would be the validation over not healthy population such as some cases of dementia, brain tumors and multiple sclerosis. This further validation has been planned for future works.

REFERENCES

[1] Liao, M., Yang, W., Zhang, X., Lu, M., and Dou, W., "A preprocessing method for magnetic resonance images of head to improve the performance of brain extraction tools," in [*Biomedical Engineering and Informatics (BMEI), 2014 7th International Conference on*], 121–125, IEEE (2014).

[2] Wang, Y., Nie, J., Yap, P.-T., Li, G., Shi, F., Geng, X., Guo, L., Shen, D., Initiative, A. D. N., et al., "Knowledge-guided robust mri brain extraction for diverse large-scale neuroimaging studies on humans and non-human primates," *PloS one* **9**(1) (2014).

[3] Lee, J., "Evaluation of automated and semi-automated skull-stripping algorithms using similarity index and segmentation error," *Computers in Biology and Medicine* **33**, 495–507 (Nov. 2003).

[4] Grau, V., Mewes, A. U., Alcaniz, M., Kikinis, R., and Warfield, S. K., "Improved watershed transform for medical image segmentation using prior information," *IEEE Trans Med Imaging* **23**, 447–458 (Apr 2004).

[5] Hartley, S., Scher, A., Korf, E., White, L., and Launer, L., "Analysis and validation of automated skull stripping tools: a validation study based on 296 MR images from the Honolulu Asia aging study," *Neuroimage* **30**(4), 1179–1186 (2006).

[6] Boesen, K., Rehm, K., Schaper, K., Stoltzner, S., Woods, R., Luders, E., and Rottenberg, D., "Quantitative comparison of four brain extraction algorithms," *Neuroimage* **22**, 1255–1261 (Jul 2004).

[7] Somasundaram, K. and Kalaiselvi, T., "Automatic brain extraction methods for t1 magnetic resonance images using region labeling and morphological operations," *Computers in biology and medicine* **41**(8), 716–725 (2011).

[8] Smith, S. M., "Fast robust automated brain extraction.," *Human brain mapping* **17**, 143–55 (Nov. 2002a).

[9] Ashburner, J. and Friston, K. J., "Voxel-based morphometry–the methods," *Neuroimage* **11**, 805–821 (Jun 2000).

[10] Zhuang, A., Valentino, D., and Toga, A., "Skull-stripping magnetic resonance brain images using a model-based level set," *NeuroImage* **32**(1), 79–92 (2006).

[11] Ségonne, F., Dale, A., Busa, E., Glessner, M., Salat, D., Hahn, H., and Fischl, B., "A hybrid approach to the skull stripping problem in MRI," *Neuroimage* **22**(3), 1060–1075 (2004).

[12] Iglesias, J. E., Liu, C.-Y., Thompson, P. M., and Tu, Z., "Robust brain extraction across datasets and comparison with publicly available methods," *Medical Imaging, IEEE Transactions on* **30**(9), 1617–1634 (2011).

[13] Cox, R. W., "Afni: software for analysis and visualization of functional magnetic resonance neuroimages," *Computers and Biomedical research* **29**(3), 162–173 (1996).

[14] Iglesias, J. E., Liu, C.-Y., Thompson, P. M., and Tu, Z., "Robust brain extraction across datasets and comparison with publicly available methods.," *IEEE transactions on medical imaging* **30**, 1617–34 (Sept. 2011).

[15] Bauer, S., Fejes, T., and Reyes, M., "A skull-stripping filter for itk," *Insight Journal* (2012).

[16] Ridler, T. and Calvard, S., "Picture thresholding using an iterative selection method," *IEEE transactions on Systems, Man and Cybernetics* **8**(8), 630–632 (1978).

[17] Meegama, R. G. and Rajapakse, J. C., "Fully automated peeling technique for t1-weighted, high-quality mr head scans," *International Journal of Image and Graphics* **4**(02), 141–156 (2004).

[18] Lehmann, G., "Label object representation and manipulation with itk," *Insight Journal* (2007).

[19] Shattuck, D. W., Mirza, M., Adisetiyo, V., Hojatkashani, C., Salamon, G., Narr, K. L., Poldrack, R. A., Bilder, R. M., and Toga, A. W., "Construction of a 3d probabilistic atlas of human cortical structures," *NeuroImage* **39**(3), 1064 – 1080 (2008).

[20] Huttenlocher, D. P., Klanderman, G., Rucklidge, W. J., et al., "Comparing images using the hausdorff distance," *Pattern Analysis and Machine Intelligence, IEEE Transactions on* **15**(9), 850–863 (1993).